NASA Technical Memorandum 85766

ANALYTICAL RESULTS FOR POSTBUCKLING BEHAVIOR OF PLATES IN COMPRESSION AND IN SHEAR

MANUEL STEIN

MARCH 1984

NASA
National Aeronautics and
Space Administration

Langley Research Center
Hampton, Virginia 23665

NASA Technical Memorandum 85766

ANALYTICAL RESULTS FOR POSTBUCKLING BEHAVIOR OF PLATES IN COMPRESSION AND IN SHEAR

MANUEL STEIN

MARCH 1984

NASA
National Aeronautics and
Space Administration

Langley Research Center
Hampton, Virginia 23665

ANALYTICAL RESULTS FOR POSTBUCKLING BEHAVIOR OF PLATES IN COMPRESSION AND IN SHEAR

Manuel Stein
NASA Langley Research Center

ABSTRACT

Results are obtained which determine the postbuckling behavior of long rectangular isotropic and orthotropic plates. By assuming trigonometric functions in one direction, the nonlinear partial differential equations of von Karman large deflection plate theory are converted into nonlinear ordinary differential equations. The ordinary differential equations are solved numerically using an available boundary value problem solver which makes use of Newton's method. Results for longitudinal compression show different postbuckling behavior between isotropic and orthotropic plates. Results for shear show that change in inplane edge constraints can cause large change in postbuckling stiffness.

INTRODUCTION

The rectangular plate supported at its edges is one of the basic elements in a structure. The structural behavior of plates must be understood for a variety of loadings and structural configurations. With the recent uses of laminated filamentary composite plates in aircraft construction, technology is needed for orthotropic plates as well as isotropic plates (including quasi-isotropic layups of filamentary composite). Buckling loads for orthotropic and isotropic plates in compression and in shear have been obtained, and they are reviewed in reference 1. Although the level of loading that causes buckling is important, supported plates may be able to carry considerable load beyond buckling. Also, various constraints applied to a test specimen in the laboratory or to a plate that is part of a panel in an actual structure may result in the same or nearly the same buckling behavior, but quite different postbuckling behavior.

In reference 2 postbuckling behavior has been determined for specially orthotropic long plates loaded in longitudinal compression. The edges are simply supported or clamped. The edges are held straight with zero average transverse load, but they can displace in the longitudinal direction locally so that the shear load at the edge is zero. In reference 3 postbuckling behavior has been determined for long isotropic and ±45° laminated plates loaded in longitudinal compression, in shear, and in combined compression and shear. For the plates of reference 3 the edges are simply supported and held straight with zero average transverse load, but the edges cannot displace locally and the overall shear displacement at the edges is prescribed.

The purpose of this paper is to present the method of analysis and postbuckling results for long plates loaded in compression and in shear with constraints at the edges of the plate that might be an upper limit to the constraints expected in experiments and in actual structures. The constraint considered for both compression

and shear is the requirement that the edges remain straight and do not move toward each other. Another constraint is considered for shear in which the edges are required to remain straight and to move toward each other in the manner expected for a plate attached to a rigid frame pinned at the corners. Results for plates with these constraints are compared to results for which the average stress across the width of the plate is zero. Both simply supported and clamped edges are treated.

An extension of the method of references 2 and 3 is used to obtain the results in this paper. In this method, the equations of von Karman, which are nonlinear partial differential equations, are converted into nonlinear ordinary differential equations by assuming trigonometric functions in one direction. These equations are then solved numerically using the method of reference 4 in a special purpose computer program which is much more efficient than available general purpose computer programs for similar calculations. The effects of change in buckle pattern are included in the calculations.

ANALYSIS

Consider the analysis of a long orthotropic simply supported or clamped plate loaded in compression and in shear with the long edges held straight and fixed so that they cannot move toward each other. Also consider the same conditions for shear loading except that the edges move toward each other in the manner expected for a rigid frame pinned at the corners. Reference 3 has presented a method of analysis and a solution technique for these problems when the long edges are free to move toward each other. To study these problems with the analysis of reference 3 requires the addition of two unknowns (and two equations) to the set of simultaneous equations and changes in the boundary conditions. The derivation of reference 3 is presented here including the changes required for application to the present problem.

A sketch of the buckled plate loaded in compression is shown below

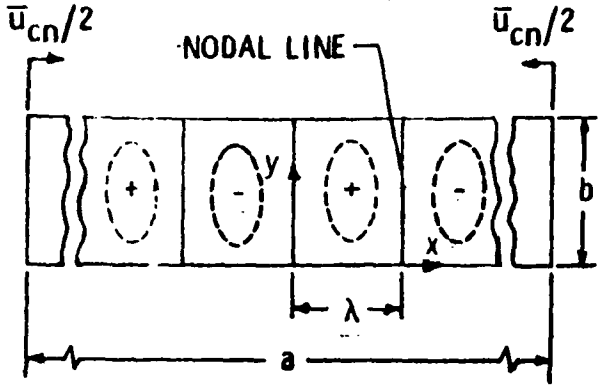

A sketch of the buckled plate loaded in shear is shown below

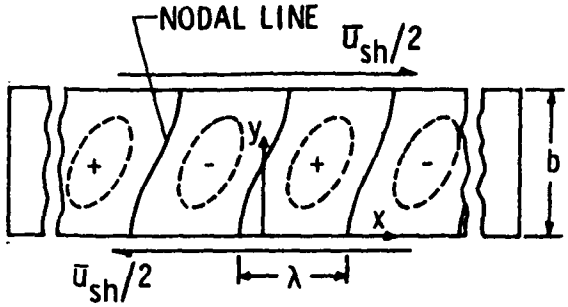

The plates have a width b and a half wavelength λ in the y and x directions, respectively. For the compression loading displacements $\bar{U}_{cn}/2$ are applied at the ends. For the shear loading, shear displacements $\bar{U}_{sh}/2$ are applied at the long edges $y = 0, b$. The out of plate deflection w is zero at the nodes of the buckle pattern (every half-wavelength) and is zero at the edges $y = 0, b$.

Displacements.- Nonlinear ordinary differential equations are derived based on a trigonometric series approximation for the displacements. The terms in the trigonometric series that are chosen are based on the exact terms required for prebuckling and buckling and a few terms beyond as suggested by a perturbation method (see, for example, ref. 5). The displacements chosen follow and are appropriate for compression, for shear, and for a combination of compression and shear (see reference 3).

$$u = -\bar{u}_{cn}\left(\frac{x}{a} - \frac{1}{2}\right) + u_0(y) + u_s(y)\sin\frac{2\pi x}{\lambda} + u_c(y)\cos\frac{2\pi x}{\lambda}$$

$$v = v_0(y) + v_s(y)\sin\frac{2\pi x}{\lambda} + v_c(y)\cos\frac{2\pi x}{\lambda} \qquad (1)$$

$$w = w_s(y)\sin\frac{\pi x}{\lambda} + w_c(y)\cos\frac{\pi x}{\lambda}$$

The deflection w, which is exact at buckling, is sinusoidally periodic with half-wavelength λ. The displacements u and v are sinusoidally periodic with half-wavelength $\lambda/2$, and u has an extra, linear-in-x, term associated with the constant $\bar{u}_{cn}$ which is specified. Specifying $\bar{u}_{cn}$ identifies the applied longitudinal compressive displacement. The applied shearing displacement $\bar{u}_{sh}$ is specified through boundary conditions on $u_o(y)$.

Derivation of differential equations.- The neutral surface strains and curvatures as given by von Karman are

$$\epsilon_x = \frac{\partial u}{\partial x} + \frac{1}{2}\left(\frac{\partial w}{\partial x}\right)^2$$
$$\epsilon_y = \frac{\partial v}{\partial y} + \frac{1}{2}\left(\frac{\partial w}{\partial y}\right)^2$$
$$\gamma_{xy} = \frac{\partial u}{\partial y} + \frac{\partial v}{\partial x} + \frac{\partial w}{\partial x}\frac{\partial w}{\partial y}$$
$$K_x = -\frac{\partial^2 w}{\partial x^2}$$
$$K_y = -\frac{\partial^2 w}{\partial y^2}$$
$$K_{xy} = -2\frac{\partial^2 w}{\partial x \partial y}$$

By substitution from equation 1, the strains and curvatures are of the form

$$\epsilon_x = \epsilon_{xo}(y) + \epsilon_{xs}(y)\sin\frac{2\pi x}{\lambda} + \epsilon_{xc}(y)\cos\frac{2\pi x}{\lambda}$$
$$\epsilon_y = \epsilon_{yo}(y) + \epsilon_{ys}(y)\sin\frac{2\pi x}{\lambda} + \epsilon_{yc}(y)\cos\frac{2\pi x}{\lambda}$$
$$\gamma_{xy} = \gamma_{xyo}(y) + \gamma_{xys}(y)\sin\frac{2\pi x}{\lambda} + \gamma_{xyc}(y)\cos\frac{2\pi x}{\lambda} \qquad (2)$$
$$K_x = K_{xs}(y)\sin\frac{\pi x}{\lambda} + K_{xc}(y)\cos\frac{\pi x}{\lambda}$$
$$K_y = K_{ys}(y)\sin\frac{\pi x}{\lambda} + K_{yc}(y)\cos\frac{\pi x}{\lambda}$$
$$K_{xy} = K_{xys}(y)\sin\frac{\pi x}{\lambda} + K_{xyc}(y)\cos\frac{\pi x}{\lambda}$$

where

$$\epsilon_{xo} = -\frac{\bar{u}_{cn}}{a} + \frac{1}{4}\left(\frac{\pi}{\lambda}\right)^2 (w_s^2 + w_c^2)$$

$$\epsilon_{xs} = -\frac{2\pi}{\lambda} u_c - \frac{1}{2}\left(\frac{\pi}{\lambda}\right)^2 w_s w_c$$

$$\epsilon_{xc} = \frac{2\pi}{\lambda} u_s + \frac{1}{4}\left(\frac{\pi}{\lambda}\right)^2 (w_s^2 - w_c^2)$$

$$\epsilon_{yo} = v_o' + \frac{1}{4}(w_s'^2 + w_c'^2)$$

$$\epsilon_{ys} = v_s' + \frac{1}{2} w_s' w_c'$$

$$\epsilon_{yc} = v_c' + \frac{1}{4}(-w_s'^2 + w_c'^2)$$

$$\gamma_{xyo} = u_o' + \frac{1}{2}\frac{\pi}{\lambda}(w_s w_c' - w_c w_s') \quad (3)$$

$$\gamma_{xys} = u_s' - \frac{2\pi}{\lambda} v_c + \frac{1}{2}\frac{\pi}{\lambda}(w_s w_s' - w_c w_c')$$

$$\gamma_{xyc} = u_c' + \frac{2\pi}{\lambda} v_s + \frac{1}{2}\frac{\pi}{\lambda}(w_s w_c' + w_c w_s')$$

$$K_{xs} = \left(\frac{\pi}{\lambda}\right)^2 w_s$$

$$K_{xc} = \left(\frac{\pi}{\lambda}\right)^2 w_c$$

$$K_{ys} = -w_s''$$

$$K_{yc} = -w_c''$$

$$K_{xys} = 2\frac{\pi}{\lambda} w_c'$$

$$K_{xyc} = -2\frac{\pi}{\lambda} w_s'$$

Prime (') indicates derivative with respect to y. From the stress-strain relations for an orthotropic plate, the stress and moment resultants are

$$N_x = A_{11}\epsilon_x + A_{12}\epsilon_y$$

$$N_y = A_{22}\epsilon_y + A_{12}\epsilon_x$$

$$N_{xy} = A_{66}\gamma_{xy} \quad (4)$$

$$M_x = D_{11}K_x + D_{12}K_y$$

$$M_y = D_{22}K_y + D_{12}K_x$$

$$M_{xy} = D_{66}K_{xy}$$

The form of the stress and moment resultants in terms of the trigonometric terms in the x-direction with coefficients functions of y is similar to the form of the strains.

The virtual work of the system is

$$\delta\Pi = \int_0^b \int_0^\lambda (N_x \delta\epsilon_x + N_y \delta\epsilon_y + N_{xy} \delta\gamma_{xy} + M_x \delta\kappa_x + M_y \delta\kappa_y + M_{xy} \delta\kappa_{xy})\, dx\, dy \quad (5)$$

Substituting (2) into (5) and integrating over x results in

$$\begin{aligned}\delta\Pi = \frac{\lambda}{2} \int_0^b (&2N_{xo} \delta\epsilon_{xo} + N_{xs} \delta\epsilon_{xs} + N_{xc} \delta\epsilon_{xc} \\ &+ 2N_{yo} \delta\epsilon_{yo} + N_{ys} \delta\epsilon_{ys} + N_{yc} \delta\epsilon_{yc} \\ &+ 2N_{xyo} \delta\gamma_{xyo} + N_{xys} \delta\gamma_{xys} + N_{xyc} \delta\gamma_{xyc} \\ &+ M_{xs} \delta\kappa_{xs} + M_{xc} \delta\kappa_{xc} \\ &+ M_{ys} \delta\kappa_{ys} + M_{yc} \delta\kappa_{yc} \\ &+ M_{xys} \delta\kappa_{xys} + M_{xyc} \delta\kappa_{xyc})\, dy \end{aligned} \quad (6)$$

Substituting (3) into (6) and integrating by parts leads to

$$\begin{aligned}\delta\Pi = \frac{\lambda}{2} \int_0^b \Big\{ &-2N'_{xyo} \delta u_o + \left(-N'_{xys} + \frac{2\pi}{\lambda} N_{xc}\right) \delta u_s \\ &+ \left(-N'_{xyc} - \frac{2\pi}{\lambda} N_{xs}\right) \delta u_c - 2N'_{yo} \delta v_o \\ &+ \left(-N'_{ys} + \frac{2\pi}{\lambda} N_{xyc}\right) \delta v_s + \left(-N'_{yc} - \frac{2\pi}{\lambda} N_{xys}\right) \delta v_c \\ &+ \left[-Q'_s + \left(2N_{xo} w_s - N_{xs} w_c + N_{xc} w'_s\right) \frac{1}{2} \left(\frac{\pi}{\lambda}\right)^2 \right. \\ &+ \left(2N_{xyo} \beta_c + N_{xys} \beta_s + N_{xyc} \beta_c\right) \frac{1}{2} \frac{\pi}{\lambda} \\ &\left. + M_{xs} \left(\frac{\pi}{\lambda}\right)^2 \right] \delta w_s + \left[-Q'_c \right. \\ &+ \left(2N_{xo} w_c - N_{xs} w_s - N_{xc} w_c\right) \frac{1}{2} \left(\frac{\pi}{\lambda}\right)^2 \\ &\left. + \left(-2N_{xyo} \beta_s - N_{xys} \beta_c + N_{xyc} \beta_s\right) \frac{1}{2} \frac{\pi}{\lambda} \right. \end{aligned} \quad (7)$$

$$+ M_{xc}\left(\frac{\pi}{\lambda}\right)^2 \Big] \delta w_c \Big\} dy$$

$$+ \frac{\lambda}{2}\Big(2N_{xyo}\,\delta u_o + N_{xys}\,\delta u_s + N_{xyc}\,\delta u_c$$

$$+ 2N_{yo}\,\delta v_o + N_{ys}\,\delta v_s + N_{yc}\,\delta v_c$$

$$+ Q_s\,\delta w_s + Q_c\,\delta w_c$$

$$- M_{ys}\,\delta\beta_s - M_{yc}\,\delta\beta_c\Big)_0^b$$

where, by definition,

$$Q_s = (2N_{yo}\beta_s + N_{ys}\beta_c - N_{yc}\beta_s)\tfrac{1}{2}$$
$$+ (-2N_{xyo}w_c + N_{xys}w_s + N_{xyc}w_c)\tfrac{1}{2}\tfrac{\pi}{\lambda}$$
$$+ M'_{ys} - 2M_{xyc}\tfrac{\pi}{\lambda}$$
$$Q_c = (2N_{yo}\beta_c + N_{ys}\beta_s + N_{yc}\beta_c)\tfrac{1}{2} \qquad (8)$$
$$+ (2N_{xyo}w_s - N_{xys}w_c + N_{xyc}w_s)\tfrac{1}{2}\tfrac{\pi}{\lambda}$$
$$+ M'_{yc} + 2M_{xys}\tfrac{\pi}{\lambda}$$
$$\beta_s = w'_s$$
$$\beta_c = w'_c$$

Thus, the principle of virtual work requires satisfaction of the following differential equations and choice of boundary conditions.

$$N'_{xyo} = 0 \qquad N'_{xys} = \tfrac{2\pi}{\lambda}N_{xc} \qquad N'_{xyc} = -\tfrac{2\pi}{\lambda}N_{xs}$$
$$N'_{yo} = 0, \qquad N'_{ys} = \tfrac{2\pi}{\lambda}N_{xyc} \qquad N'_{yc} = -\tfrac{2\pi}{\lambda}N_{xys}$$
$$Q'_s = (2N_{xo}w_s - N_{xs}w_c + N_{xc}w_s)\tfrac{1}{2}\left(\tfrac{\pi}{\lambda}\right)^2$$
$$+ (2N_{xyo}\beta_c + N_{xys}\beta_s + N_{xyc}\beta_c)\tfrac{1}{2}\tfrac{\pi}{\lambda}$$
$$+ M_{xs}\left(\tfrac{\pi}{\lambda}\right)^2 \qquad (9)$$

$$Q_c' = (2N_{xo}w_c - N_{xs}w_s - N_{xc}w_c)\tfrac{1}{2}\left(\frac{\pi}{\lambda}\right)^2 + (-2N_{xyo}\beta_s - N_{xys}\beta_c + N_{xyc}\beta_s)\tfrac{1}{2}\frac{\pi}{\lambda} + M_{xc}\left(\frac{\pi}{\lambda}\right)^2$$

$$\left(N_{xyo}\delta u_o\right)_0^b = 0 \quad \left(N_{xys}\delta u_s\right)_0^b = 0 \quad \left(N_{xyc}\delta u_c\right)_0^b = 0$$

$$\left(N_{yo}\delta v_o\right)_0^b = 0 \quad \left(N_{ys}\delta v_s\right)_0^b = 0 \quad \left(N_{yc}\delta v_c\right)_0^b = 0$$

$$\left(Q_s\delta w_s\right)_0^b = 0 \quad \left(Q_c\delta w_c\right)_0^b = 0$$

$$\left(M_{ys}\delta\beta_s\right)_0^b = 0 \quad \left(M_{yc}\delta\beta_c\right)_0^b = 0$$

The boundary conditions assumed for the results presented in this paper are that the edges are held straight and either simply supported or clamped. The edge at $y = 0$ is displaced relative to the edge at $y = b$ to give a specified (applied) shearing displacement $\bar{u}_{sh}$. This displacement may be applied through a rigid frame pinned at the corners of the plate. However, this kind of frame also applies a compressive displacement across the width equal to $b - \sqrt{b^2 - \bar{u}_{sh}^2}$ which is given, to sufficient accuracy, by $\bar{u}_{sh}^2/(2b)$. The boundary condition that v is equal to zero at the edges is considered for compression loading and it is also considered for shear loading instead of the rigid frame condition.

These boundary conditions are expressed as follows:

Simply supported or clamped at $y = 0,b$	$w_s = w_c = 0$ and
	$M_{ys} = M_{yc} = 0$ or $\beta_s = \beta_c = 0$
Straight edges at $y = 0,b$	$u_s = u_c = v_s = v_c = 0$
Applied shearing displacement at $y = 0$	$u_o = -\bar{u}_{sh}/2$,
$y = b$	$u_o = \bar{u}_{sh}/2$

In addition, for shear loading, there may be transverse compressive displacements, due to a rigid frame, at

$$y = 0 \qquad v_o = -\bar{u}_{sh}^2/(4b)$$

$$y = b \qquad u_o = \bar{u}_{sh}^2/(4b)$$

or, instead, for both compression and shear loading the edges are constrained so that they do not move together or apart, at

$$y = 0,\ b \qquad v_o = 0$$

The system of first order ordinary differential equations to be solved for this problem are presented in terms of the 20 unknowns

$$u_o, u_s, u_c, v_o, v_s, v_c, w_s, w_c, \beta_s, \beta_c$$

$$N_{xyo}, N_{xys}, N_{xyc}, N_{yo}, N_{ys}, N_{yc}, Q_s, Q_c, M_{ys}, M_{yc}$$

Equations (9), which were obtained from the virtual work, present eight of the system of differential equations used. Equations (10), which follow, were obtained from the stress-strain relations (4) using equations (2), (3), and (8); they present eight more differential equations

$$u_o' = -\tfrac{1}{2}\tfrac{\pi}{\lambda}\left(w_s\beta_c - w_c\beta_s\right) + N_{xyo}/A_{66}$$

$$u_s' = \tfrac{2\pi}{\lambda}v_c - \tfrac{1}{2}\tfrac{\pi}{\lambda}\left(w_s\beta_s - w_c\beta_c\right) + N_{xys}/A_{66}$$

$$u_c' = -\tfrac{2\pi}{\lambda}v_s - \tfrac{1}{2}\tfrac{\pi}{\lambda}\left(w_s\beta_c + w_c\beta_s\right) + N_{xyc}/A_{66}$$

$$v_o' = -\tfrac{1}{4}\left(\beta_s^2 + \beta_c^2\right) - A_{12}/A_{22}\left[-\frac{\bar{u}_{cn}}{a} + \tfrac{1}{4}\left(\tfrac{\pi}{\lambda}\right)^2\left(w_s^2 + w_c^2\right)\right] + N_{yo}/A_{22}$$

$$v_s' = -\tfrac{1}{2}\beta_s\beta_c + \left(A_{12}/A_{22}\right)\left[\tfrac{2\pi}{\lambda}u_c + \tfrac{1}{2}\left(\tfrac{\pi}{\lambda}\right)^2 w_s w_c\right] + N_{ys}/A_{22} \qquad (10)$$

$$v_c' = \tfrac{1}{4}\left(\beta_s^2 - \beta_c^2\right) - \left(A_{12}/A_{22}\right)\left[\tfrac{2\pi}{\lambda}u_s + \tfrac{1}{4}\left(\tfrac{\pi}{\lambda}\right)^2\left(w_s^2 - w_c^2\right)\right] + N_{yc}/A_{22}$$

$$\beta_s' = \left(D_{12}/D_{22}\right)\left(\tfrac{\pi}{\lambda}\right)^2 w_s - M_{ys}/D_{22}$$

$$\beta_c' = \left(D_{12}/D_{22}\right)\left(\tfrac{\pi}{\lambda}\right)^2 w_c - M_{yc}/D_{22}$$

Four differential equations result from the definitions (8)

$$w_s' = \beta_s$$

$$w_c' = \beta_c$$

$$M_{ys}' = Q_s - (2N_{yo}\beta_s + N_{ys}\beta_c - N_{yc}\beta_s)\tfrac{1}{2} - (-2N_{xyo}w_c + N_{xys}w_s + N_{xyc}w_c)\tfrac{1}{2}\tfrac{\pi}{\lambda} + M_{xyc}\tfrac{2\pi}{\lambda} \qquad (11)$$

$$M_{yc}' = Q_c - (2N_{yo}\beta_c + N_{ys}\beta_s + N_{yc}\beta_c)\tfrac{1}{2} - (2N_{xyo}w_s - N_{xys}w_c + N_{xyc}w_s)\tfrac{1}{2}\tfrac{\pi}{\lambda} - M_{xys}\tfrac{2\pi}{\lambda}$$

The following additional relations are needed, they were also obtained from the stress-strain relations (4) using equations (2), (3) and (8)

$$N_{xo} = (A_{11} - A_{12}^2/A_{22})\left[-\frac{\bar{u}_{cn}}{a} + \tfrac{1}{4}\left(\tfrac{\pi}{\lambda}\right)^2(w_s^2 + w_c^2)\right] + (A_{12}/A_{22})N_{yo}$$

$$N_{xs} = -(A_{11} - A_{12}^2/A_{22})\left[u_c\tfrac{2\pi}{\lambda} + \tfrac{1}{2}\left(\tfrac{\pi}{\lambda}\right)^2 w_s w_c\right] + (A_{12}/A_{22})N_{ys}$$

$$N_{xc} = (A_{11} - A_{12}^2/A_{22})\left[u_s\tfrac{2\pi}{\lambda} + \tfrac{1}{4}\left(\tfrac{\pi}{\lambda}\right)^2(w_s^2 - w_c^2)\right] + (A_{12}/A_{22})N_{yc} \qquad (12)$$

$$M_{xs} = (D_{11} - D_{12}^2/D_{22})\left(\tfrac{\pi}{\lambda}\right)^2 w_s + (D_{12}/D_{22})M_{ys}$$

$$M_{xc} = (D_{11} - D_{12}^2/D_{22})\left(\tfrac{\pi}{\lambda}\right)^2 w_c + (D_{12}/D_{22})M_{yc}$$

$$M_{xys} = \tfrac{2\pi}{\lambda} D_{66}\beta_c$$

$$M_{xyc} = -\tfrac{2\pi}{\lambda} D_{66}\beta_s$$

In summary, nonlinear ordinary differential equations have been derived from basic relations, by using simplifying assumptions, to replace the nonlinear partial differential equations of plate theory. The derivation employed the principle of virtual work in conjunction with the assumption that the displacements are represented by the first few terms of a Fourier series. Solution of the ordinary differential equations, subject to the boundary conditions which arise naturally in the derivation, is obtained using the algorithm described in the next paragraph.

Solution technique.- An algorithm based on Newton's method has been developed by Lentini and Pereyra in reference 4 to solve a system of simultaneous first order nonlinear ordinary differential equations subject to two point boundary conditions. The system of equations is of the form

$$\bar{y}' = \bar{F}(x,\bar{y})$$

where $\bar{y}$ is the vector of dependent variables and x is the independent variable defined in the interval (a,b). The boundary conditions of the problem are specified by

$$\bar{g}\ (\bar{y}(a),\ \bar{y}(b)) = 0$$

This algorithm uses finite differences with deferred corrections, and adaptive mesh spacings are automatically produced so that mild boundary layers are detected and resolved.

Applications

This paper presents results for a long plate loaded in longitudinal compression and in inplane shear beyond its buckling load. For given values of the applied displacements $\bar{u}_{cn}$ and $\bar{u}_{sh}$ and for prescribed values of the dimensions, material properties, and half-wavelength λ, the system of equations may be solved and the average compressive stress intensity and shear stress intensity may be determined, where the average stress intensities are

$$N_{xav} = \frac{-1}{2\lambda b}\int_0^b \int_0^{2\lambda} N_x \, dx\, dy = -\frac{1}{b}\int_0^b N_{xo}\, dy$$

$$N_{xyav} = \frac{1}{2\lambda b}\int_0^b \int_0^{2\lambda} N_{xy}\, dx\, dy = N_{xyo}$$

The wavelength of interest is the one that corresponds to minimum energy, and the solution of interest is on the equilibrium path that gives nonzero deflections.

Results are obtained for isotropic and ±45° laminated composite plates with a balanced and symmetric layup. The isotropic results apply to isotropic metal or composites with a quasi-isotropic layup. The ±45° laminate results apply to graphite-epoxy filamentary material with properties given by the dimensionless quantities

$$\frac{D_{12} + 2D_{66}}{\sqrt{D_{11}D_{22}}} = 2.28$$

$$\frac{A_{11}A_{22} - A_{12}^2 - 2A_{12}A_{66}}{2A_{66}\sqrt{A_{11}A_{22}}} = -.431$$

For the isotropic plate both of these quantities are unity, and for both the isotropic and ±45° laminate

$$\frac{A_{22}D_{11}}{A_{11}D_{22}} = 1$$

These parameters are discussed in reference 2.

Results and Discussion

Characteristic load-displacement curves for the postbuckling behavior of long isotropic plates loaded in longitudinal compression are plotted in figure 1. The long edges are either simply supported or clamped and held straight with either the average transverse stress intensity equal to zero or the displacement equal to zero normal to the long edges. The average longitudinal compressive stress intensity coefficient is plotted as a function of the applied compressive displacement coefficient. The

curves for zero average stress and zero displacement edge conditions cross for simply supported and for clamped edges. The slope of these curves indicate that in the postbuckling range plates with clamped edges are stiffer than plates with simply supported edge and that plates with the zero displacement edge condition are stiffer than corresponding plates with the zero average stress condition. The average transverse stress intensity for the zero displacement edge condition is presented in figure 2. This average stress is normalized with respect to the column buckling stress of a wide plate and this normalized stress is plotted as a function of the applied displacement normalized with respect to the longitudinal buckling displacement. As the plate is compressed along the length, compressive stresses develop across the width because the plate is not free to expand until the plate buckles under combined loading. After buckling these compressive stresses across the width are relieved and in the postbuckling range tensile stresses appear for the isotropic plate.

Characteristic load-displacement curves for the postbuckling behavior of long ±45° laminated composite plates loaded in longitudinal compression are plotted in figure 3, and curves for average transverse stress intensity for this plate are plotted in figure 4. These results are calculated for the same boundary conditions as for the isotropic plates. The trends in figure 3 are similar to those of figure 1 and the slopes of curves indicate that the isotropic plate is slightly stiffer than the ±45° laminate.

The compressive stresses across the width increase after buckling at a slower rate for the ±45° laminate as shown in figure 4 instead of dropping off and going into tension as shown in figure 2 for the isotropic plate. The transverse tension that builds up in the postbuckling range in the isotropic plate is due to a combination of shallow buckles and the zero transverse inplane deformation condition. For the ±45° laminate the buckles are deeper, and, therefore, the tension does not build up.

Characteristic load-displacement curves for the postbuckling behavior of long isotropic plates loaded in shear are plotted in figure 5. The long edges are either simply supported or clamped. The long edges are held straight and either (1) the average transverse stress intensity is zero, (2) the long edges displace toward each other as required by a rigid frame pinned at the corners, or (3) the transverse inplane displacement is zero. The average shear stress intensity coefficient is plotted as a function of the applied shear displacement coefficient. Depending on the inplane conditions the curves branch at the values of the coefficient that correspond to buckling loads for simply supported and clamped plates. The slopes of these curves indicate that in the postbuckling range plates with clamped edges are stiffer than plates with simply supported edges, and that plates with the zero displacement edge condition are stiffer than with the rigid frame, and that both of these are much stiffer than plates with average transverse stress equal to zero.

The average longitudinal stress intensity for long isotropic plates in shear is presented in figure 6 and the average transverse stress intensity is presented in figure 7. These stresses are normalized with respect to their buckling values, and the normalized stresses are plotted as a function of the applied displacement normalized with respect to the buckling displacement. Nearly independent of boundary conditions the tensile longitudinal stress increases up to about 4 times its critical value in the postbuckling range as shown in figure 6 as the shear displacement increases to 7 times its critical value. The tensile transverse stress increases up to about 17 times its critical value for the zero displacement-simply supported edge conditions in the postbuckling range shown in figure 7. These results show that for plates loaded in shear the longitudinal and transverse stresses can be very large in the postbuckling range.

Curves for the postbuckling behavior of long ±45° laminated composite plates loaded in shear are plotted in figures 8, 9, and 10. The slopes in figure 8 show

the same trends as shown for the isotropic plates in figure 5 except that they indicate that the stiffness of the ±45° laminate is less than the isotropic plates for all cases. The curves for longitudinal stress in figure 9 depend on boundary conditions whereas for the isotropic plates they did not depend on boundary conditions. The longitudinal stress is lower for the ±45° laminate for the edge condition of zero average transverse stress. The transverse stresses as given by figure 9 show similar behavior to that given for the isotropic case. The magnitude of the stresses for the ±45° laminate is higher for the transverse stresses and lower for the longitudinal stresses as compared to the isotropic plate.

CONCLUDING REMARKS

This paper presents a method of analysis and postbuckling results for long orthotropic plates loaded in longitudinal compression and in shear. Results are presented for constraints on plates which are upper limits for the behavior of experiments and actual structures. The long edges are constrained to be straight and the inplane displacement normal to the edges is equal to zero for both longitudinal compression and shear loadings. In addition, the long edges are considered to move in (normal to the edges) as required by a rigid frame pinned at the corners for shear loading. These results are compared to the case where the edges are straight but the average transverse stress is zero. All cases are for both simply supported and clamped edges and for both isotropic plates and a ±45° laminate.

Similar results are obtained for the postbuckling behavior of a plate loaded in compression for the cases of zero displacement normal to the edge and zero average transverse stress. For zero displacement normal to the edge, the transverse stress goes from compression to tension for an isotropic plate; whereas, for a ±45° laminate, the transverse stress increases in compression.

Similar results are obtained for the postbuckling behavior of a plate loaded in shear with inplane conditions appropriate to displacements normal to the edges caused by a rigid frame pinned at the corners or to zero displacement normal to the edges. The shear stiffness of a plate is much larger for the zero displacement condition than for the zero average transverse stress condition. The longitudinal stress is in tension and is large for all conditions. For an isotropic plate the average longitudinal stress normalized with respect to the critical longitudinal stress has about the same value for all boundary conditions but is lower for the zero average transverse stress condition for a ±45° laminate. The average transverse stress is very large for the isotropic plate and the ±45° laminate for the zero inplane displacement condition normal to the edges.

REFERENCES

1. Johns, D. J.: Shear Buckling of Isotropic and Orthotropic Plates--A Review. R & M No. 3677, British A.R.C., 1971.

2. Stein, Manuel: Postbuckling of Orthotropic Composite Plates Loaded in Compression. AIAA Paper No. 82-0778, 1982.

3. Stein, Manuel: Postbuckling of Long Orthotropic Plates in Combined Shear and Compression. AIAA Paper No. 83-0876, 1983.

4. Lentini, M. and Pereyra, V.: An Adaptive Finite Difference Solver for Nonlinear Two-Point Boundary Problems with Mild Boundary Layers. SIAM Journal of Numerical Analysis. Vol. 14, No. 1, March 1977.

5. Stein, M.: Loads and Deformations of Buckled Rectangular Plates. NASA TR R-40, 1959.

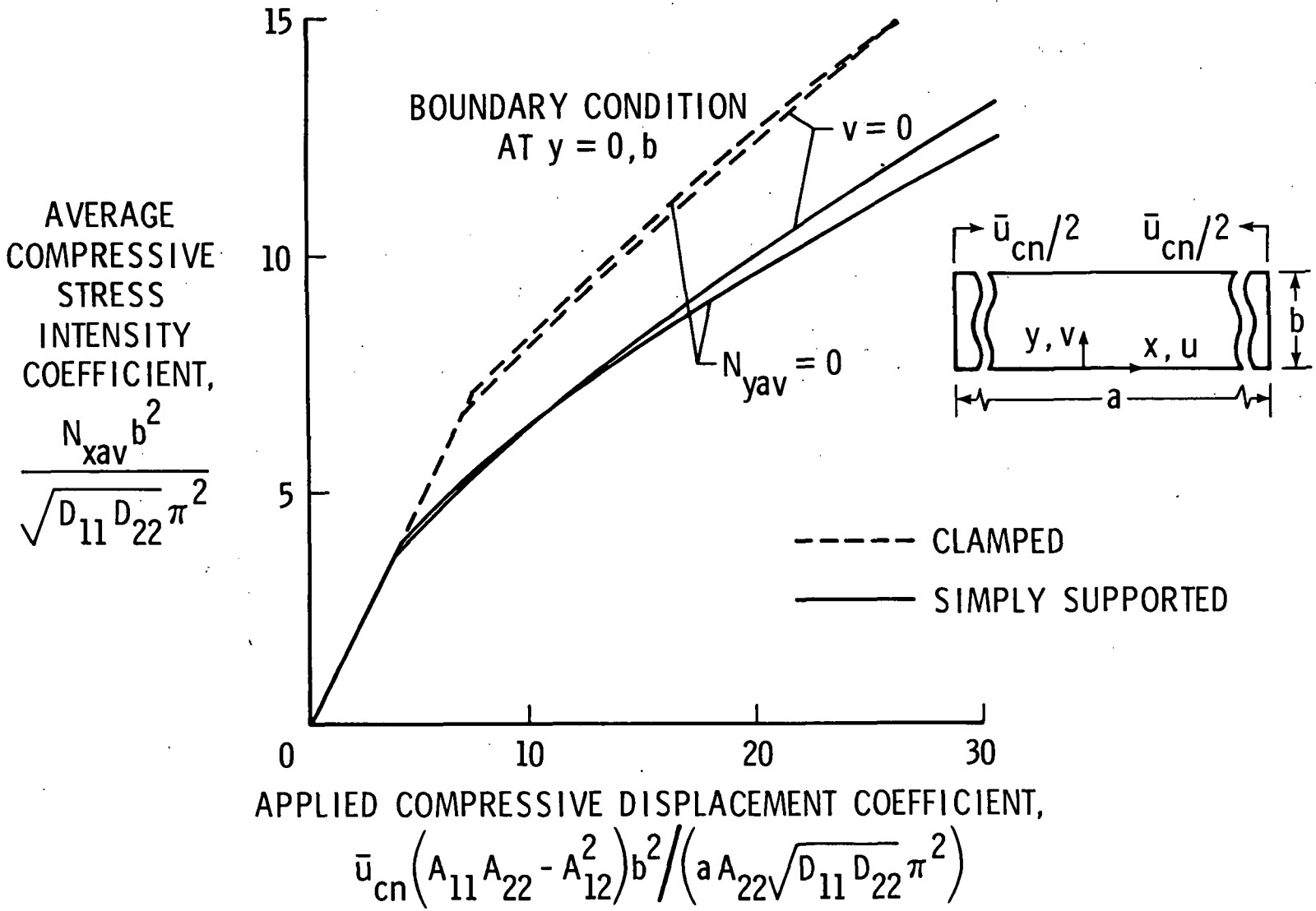

Fig. 1.- Characteristic curves for isotropic plates loaded in longitudinal compression.

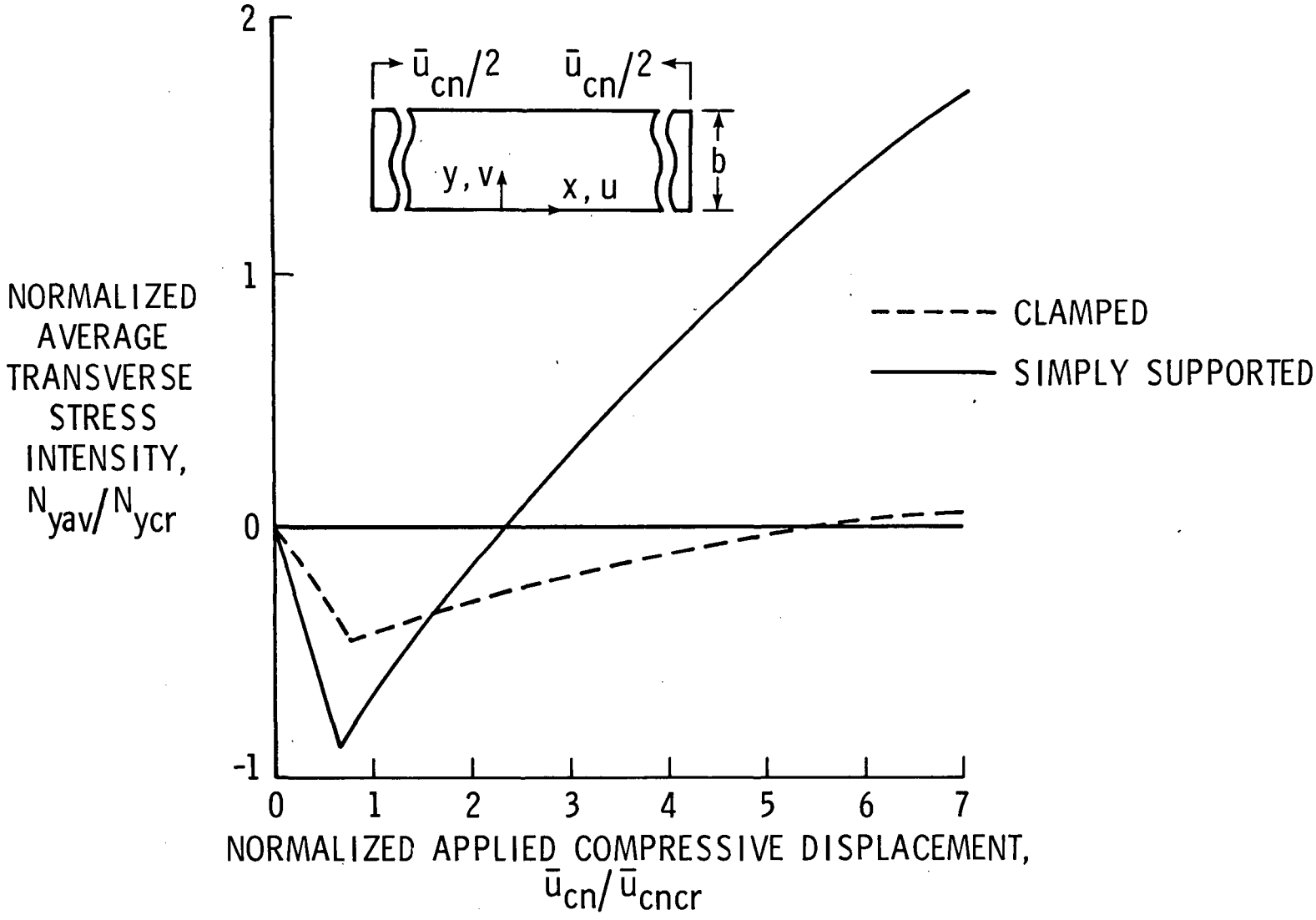

Fig. 2.- Average transverse stress for isotropic plates with zero transverse displacements, v = 0, at the edges loaded in longitudinal compression.

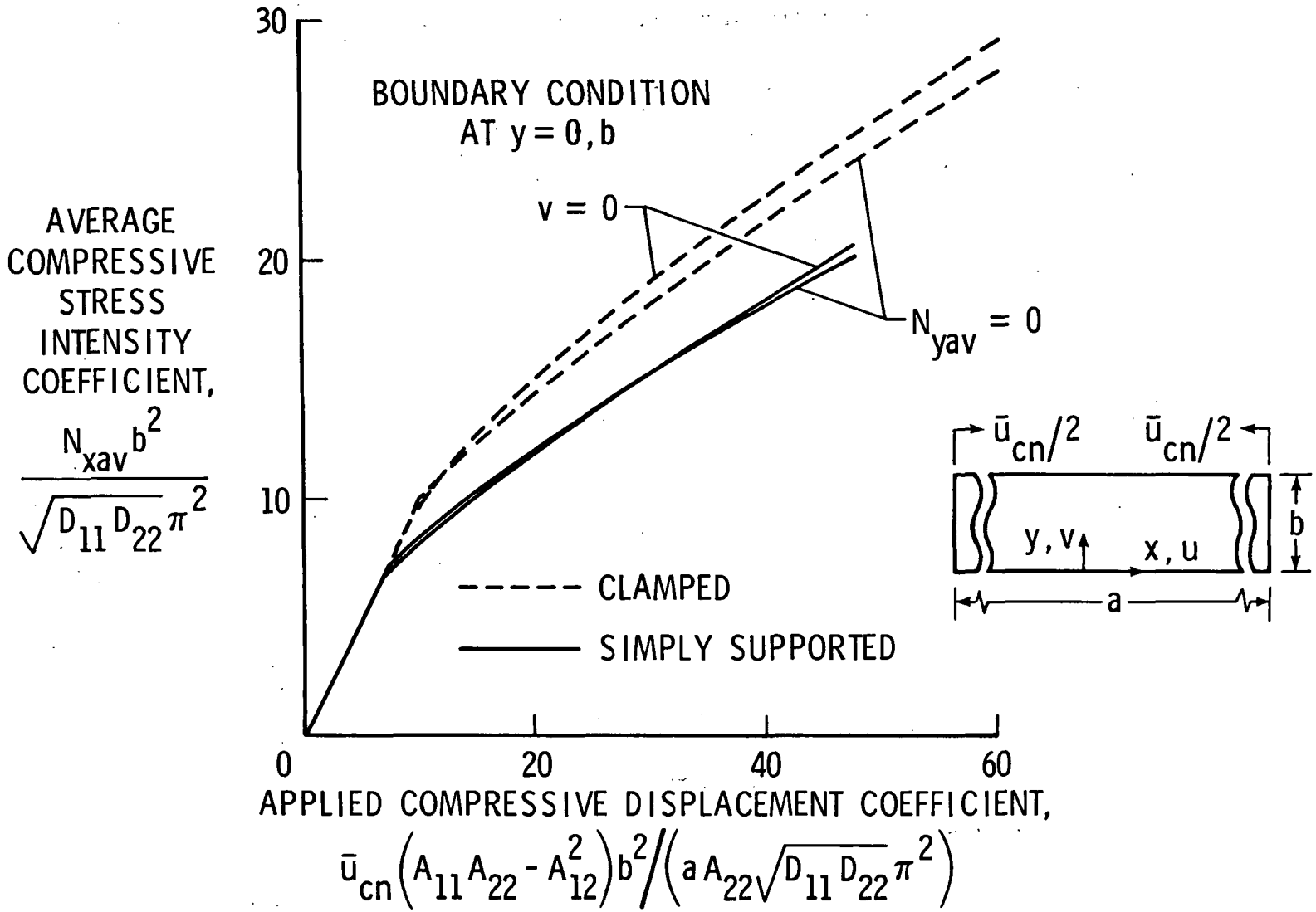

Fig. 3.- Characteristic curves for a ±45° laminated composite plate loaded in longitudinal compression.

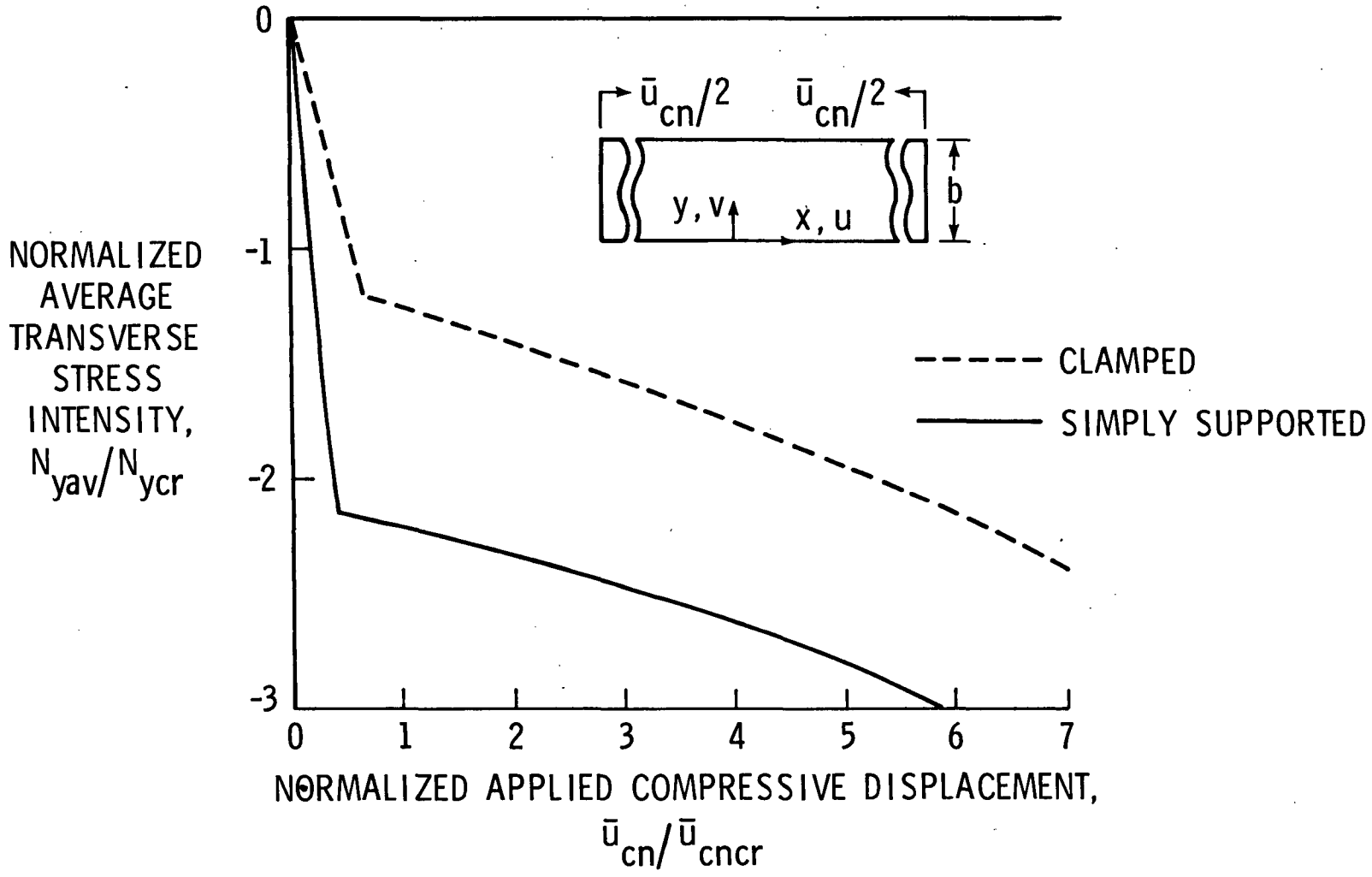

Fig. 4.- Average transverse stress for a ±45° laminated composite plate with zero transverse inplane displacements, v = 0, at the edges loaded in longitudinal compression.

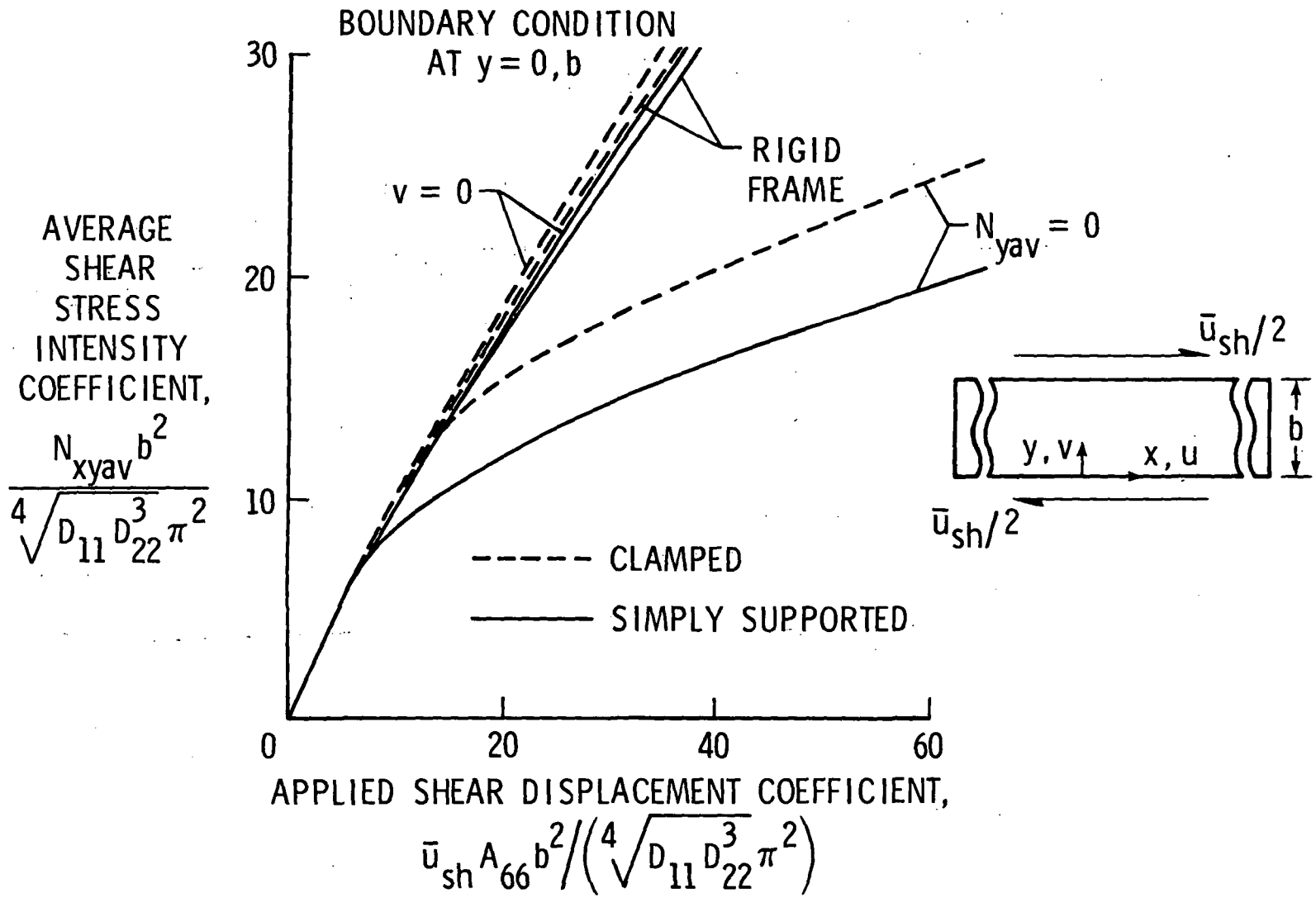

Fig. 5.- Characteristic curves for isotropic plates loaded in shear.

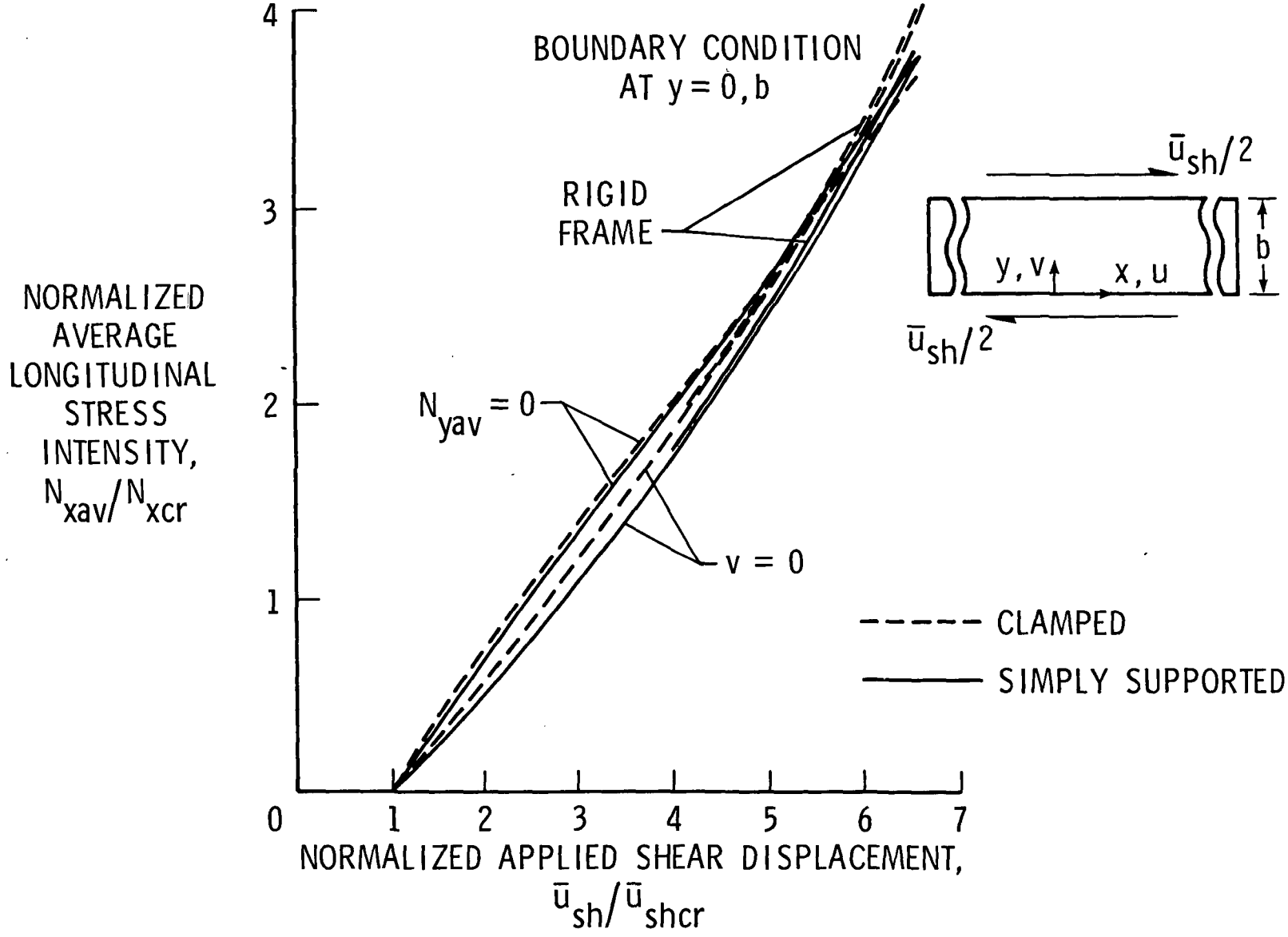

Fig. 6.- Average longitudinal stress for isotropic plates loaded in shear.

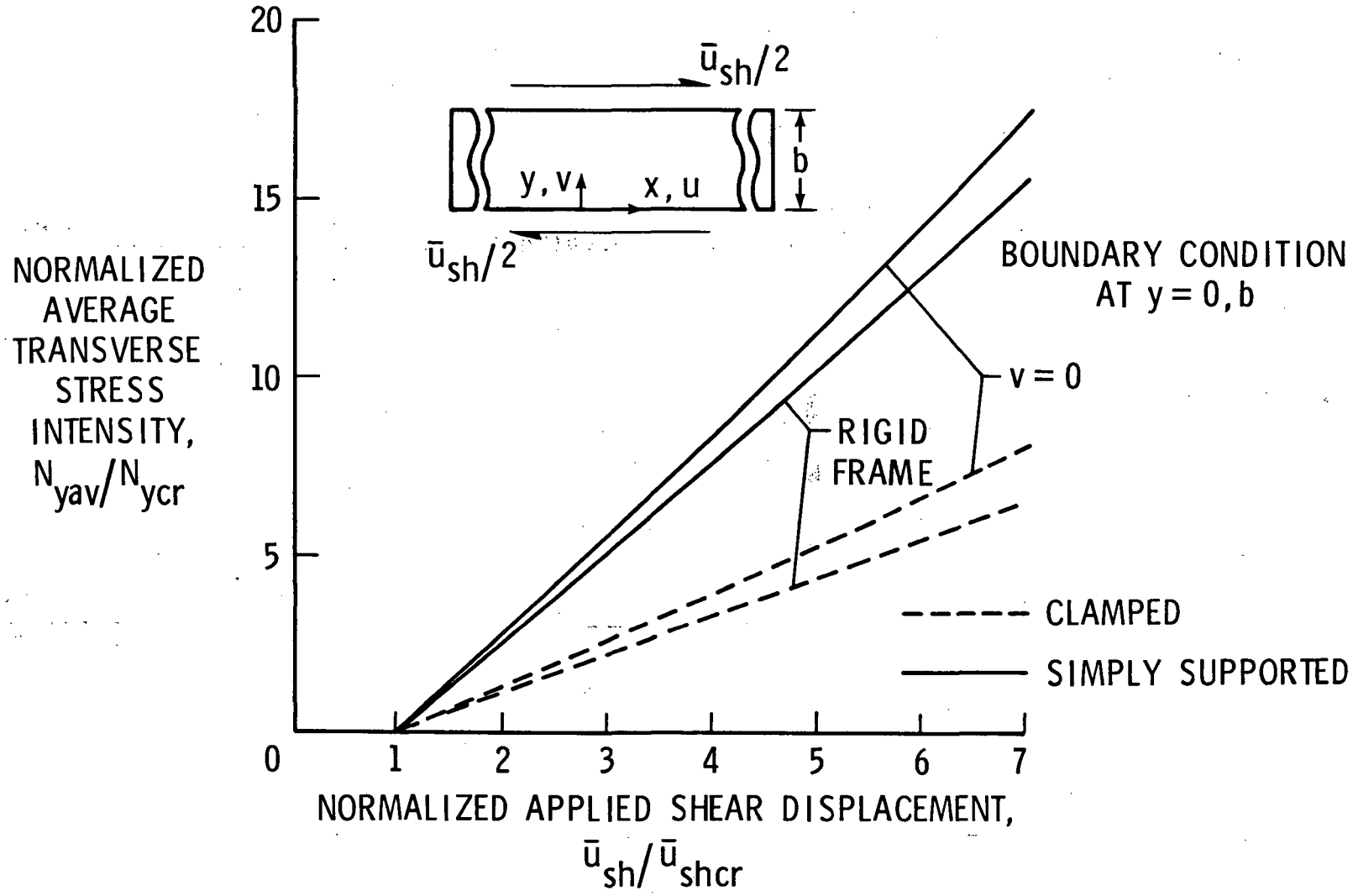

Fig. 7.- Average transverse stress for isotropic plates loaded in shear.

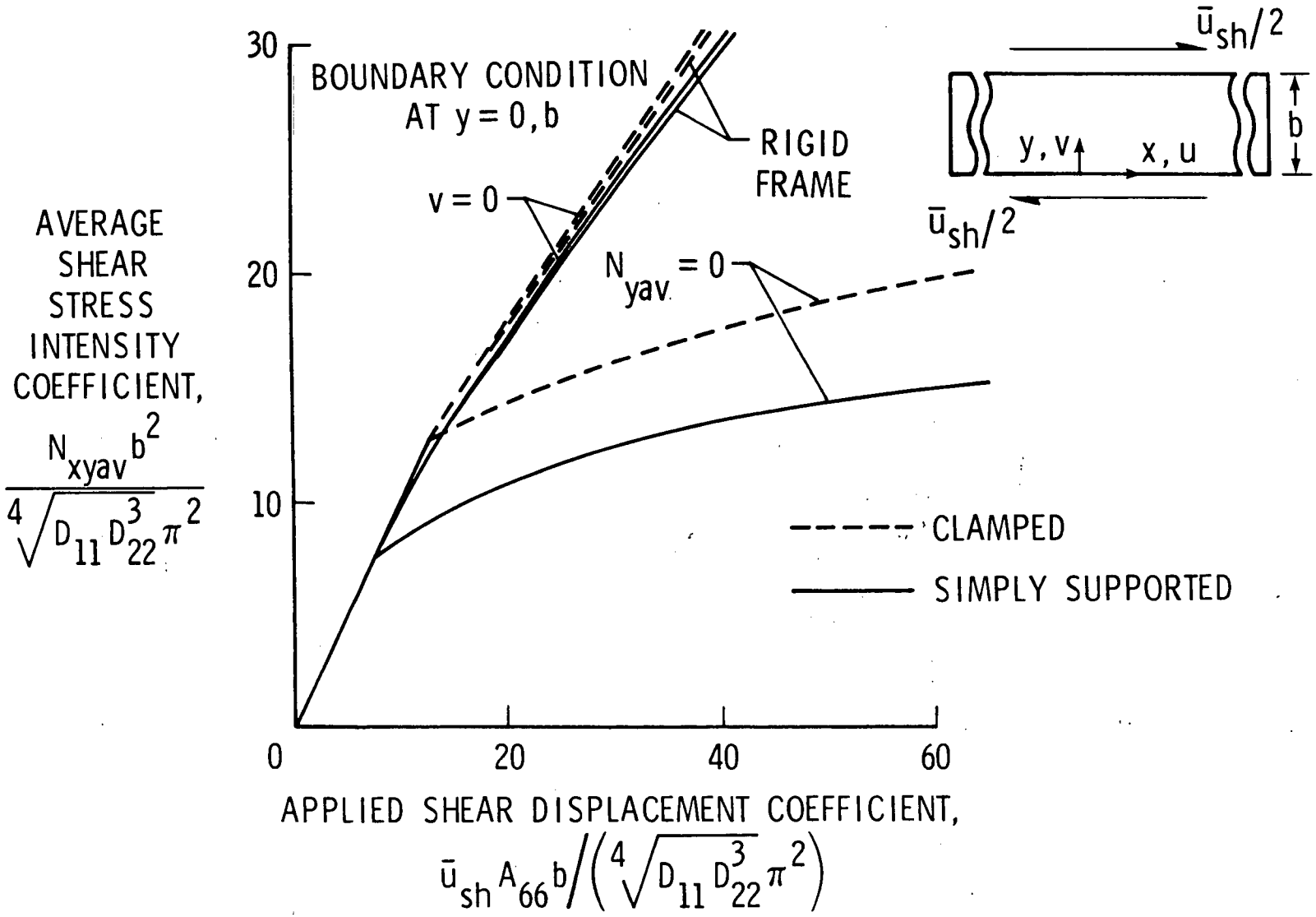

Fig. 8.- Characteristic curves for a ±45° laminated composite plate loaded in shear.

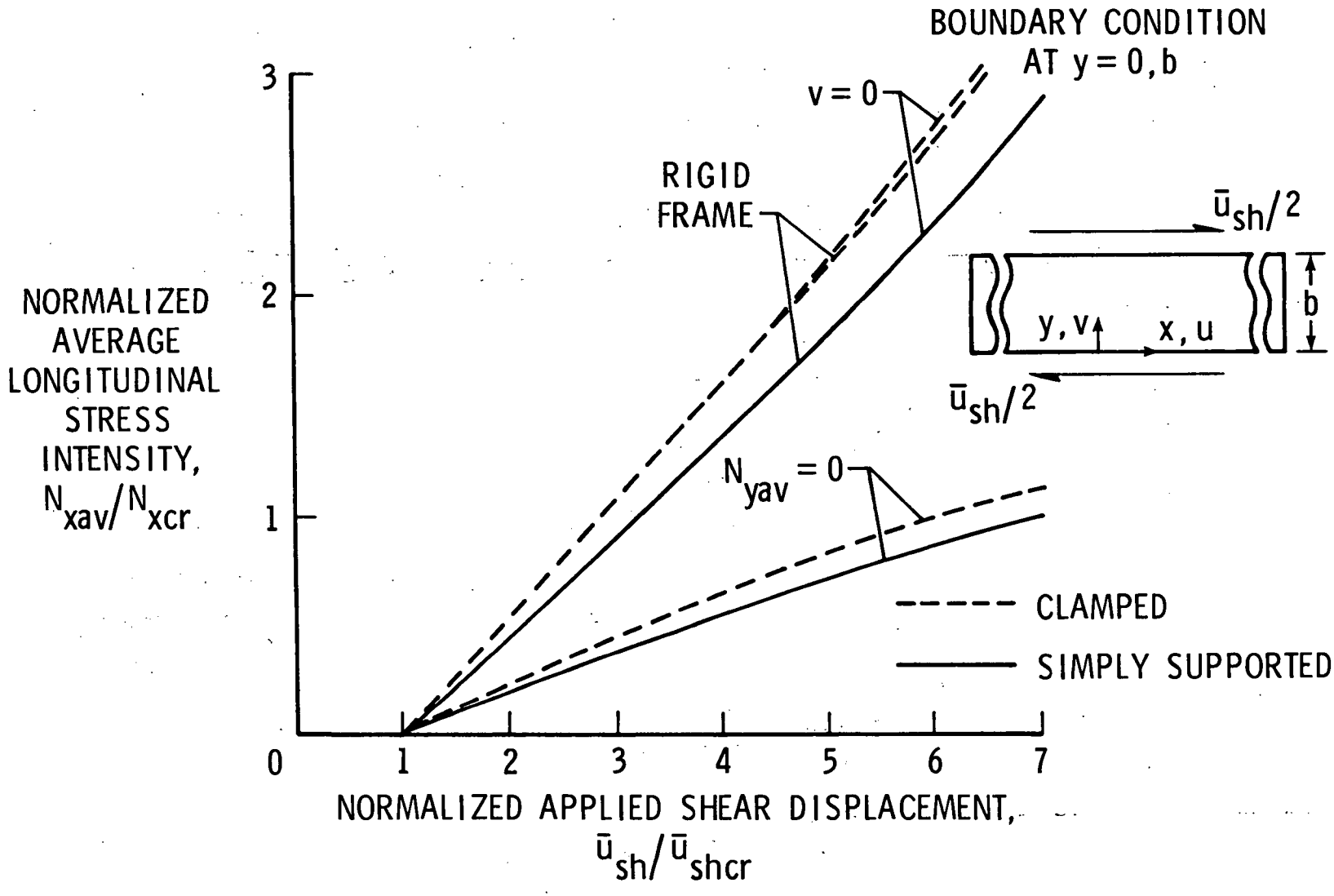

Fig. 9.- Average longitudinal stress for a ±45° laminated composite plate loaded in shear.

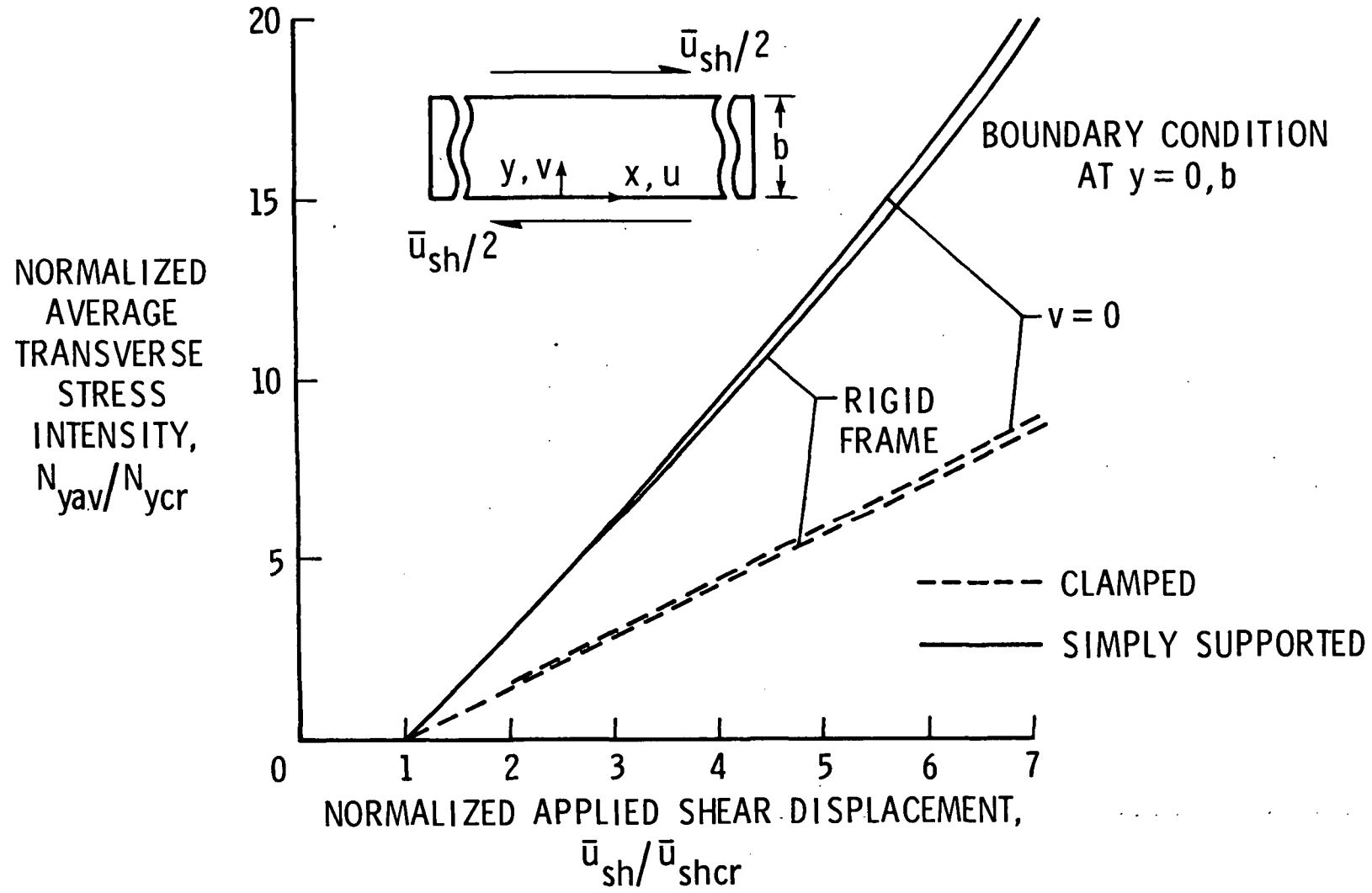

Fig. 10.- Average transverse stress for a ±45° laminated composite plate loaded in shear.

1. Report No.	2. Government Accession No.	3. Recipient's Catalog No.
NASA TM-85766		

4. Title and Subtitle	5. Report Date
Analytical Results for Postbuckling Behavior of Plates in Compression and in Shear	March 1984
	6. Performing Organization Code
7. Author(s)	8. Performing Organization Report No.
Manuel Stein	
	10. Work Unit No.
9. Performing Organization Name and Address	
NASA Langley Research Center Hampton, VA 23665	11. Contract or Grant No.
	13. Type of Report and Period Covered
12. Sponsoring Agency Name and Address	Technical Memorandum
National Aeronautics and Space Administration Washington, DC 20546	14. Sponsoring Agency Code

15. Supplementary Notes

To be published in "Aspects of the Analysis of Plate Structures," a volume in honor of W. H. Wittrick.

16. Abstract

Results are obtained which determine the postbuckling behavior of long rectangular isotropic and orthotropic plates. By assuming trigonometric functions in one direction, the nonlinear partial differential equations of von Karman large deflection plate theory are converted into nonlinear ordinary differential equations. The ordinary differential equations are solved numerically using an available boundary value problem solver which makes use of Newton's method. Results for longitudinal compression show different postbuckling behavior between isotropic and orthotropic plates. Results for shear show that change in inplane edge constraints can cause large change in postbuckling stiffness.

17. Key Words (Suggested by Author(s))	18. Distribution Statement
Postbuckling analysis rectangular plates orthotropic plates compression loading shear loading	Unclassified - Unlimited Subject Category 39

19. Security Classif. (of this report)	20. Security Classif. (of this page)	21. No. of Pages	22. Price
Unclassified	Unclassified	29	A03

For sale by the National Technical Information Service, Springfield, Virginia 22161